

AD-A238 482

ITATION PAGE

Form Approved  
OMB No 0704-0188

Estimated average 1-hour per response, including the time for reviewing instructions, searching existing data sources, gathering the collection of information, Send comments regarding this burden estimate or any other aspect of this burden to Washington Headquarters Services, Directorate for Information Operations and Reports, 1215 Jefferson Pike, Management and Budget, Paperwork Reduction Project (0704-0188), Washington, DC 20503

1. AGENCY USE ONLY (Leave blank)		2. REPORT DATE May 9, 1991	3. REPORT TYPE AND DATES COVERED Final Report	
4. TITLE AND SUBTITLE Reactions of Hydrogen Atoms Important to the Decomposition of Energetic Materials			5. FUNDING NUMBERS  DAAL03-88-K-0034	
6. AUTHOR(S)  Paul L. Houston			8. PERFORMING ORGANIZATION REPORT NUMBER	
7. PERFORMING ORGANIZATION NAME(S) AND ADDRESS(ES) Department of Chemistry Cornell University Ithaca, NY 14853-1301			10. SPONSORING/MONITORING AGENCY REPORT NUMBER  ARO 25503.1-CH	
9. SPONSORING/MONITORING AGENCY NAME(S) AND ADDRESS(ES) U. S. Army Research Office P. O. Box 12211 Research Triangle Park, NC 27709-2211			10. SPONSORING/MONITORING AGENCY REPORT NUMBER	
11. SUPPLEMENTARY NOTES The view, opinions and/or findings contained in this report are those of the author(s) and should not be construed as an official Department of the Army position, policy, or decision, unless so designated by other documentation.				
12a. DISTRIBUTION/AVAILABILITY STATEMENT  Approved for public release; distribution unlimited.			12b. DISTRIBUTION CODE	
13. ABSTRACT (Maximum 200 words)  A new technique for characterizing the velocity distributions of state-selected reaction products was developed for analyzing the reactions of hydrogen atoms: the three dimensional velocity distribution of product fragments is determined by ionizing the appropriate species, waiting for a delay while the species separate along their trajectories, and then projecting the spatial distribution of ions onto a two-dimensional screen. The objectives of this work were to develop the new technique and, eventually, to apply it to use it in order to characterize the reactions of hydrogen atoms with NO <sub>2</sub> , CH <sub>3</sub> HNO <sub>2</sub> , and H <sub>2</sub> NNO <sub>2</sub> .				
14. SUBJECT TERMS Kinetics, Molecular Dynamics, Photodissociation, Hydrogen Atoms, Energetic Materials			15. NUMBER OF PAGES 14	
			16. PRICE CODE	
17. SECURITY CLASSIFICATION OF REPORT UNCLASSIFIED	18. SECURITY CLASSIFICATION OF THIS PAGE UNCLASSIFIED	19. SECURITY CLASSIFICATION OF ABSTRACT UNCLASSIFIED	20. LIMITATION OF ABSTRACT UL	

**Best  
Available  
Copy**

Reactions of Hydrogen Atoms  
Important  
to the  
Decomposition of Energetic Materials

FINAL REPORT

Paul L. Houston

May 9, 1991

U. S. ARMY RESEARCH OFFICE

GRANT NUMBER 25503-CH

Department of Chemistry  
Cornell University  
Ithaca, NY 14853-1301

APPROVED FOR PUBLIC RELEASE;

DISTRIBUTION UNLIMITED

91-05359



Handwritten notes and stamps on the right side of the page, including a large checkmark and the text "A-1".

THE VIEWS, OPINIONS, AND/OR FINDINGS CONTAINED IN THIS REPORT ARE THOSE OF THE AUTHORS AND SHOULD NOT BE CONSTRUED AS AN OFFICIAL DEPARTMENT OF THE ARMY POSITION, POLICY, OR DECISION, UNLESS SO DESIGNATED BY OTHER DOCUMENTATION

## Table of Contents

A.	Statement of the Problem Studied .....	5
B.	Summary of the Most Important Results .....	5
1.	Apparatus Construction .....	6
2.	NO <sub>2</sub> Photodissociation .....	8
3.	CH <sub>3</sub> NO <sub>2</sub> Photodissociation .....	11
4.	Crossed Molecular Beam Apparatus .....	12
C.	List of All Publications and Technical Reports .....	13
D.	List of All Participating Scientific Personnel .....	13
E.	Report of Inventions .....	13
F.	Bibliography .....	13

## List of Figures

Figure 1. Single molecular beam apparatus used for studies of photodissociation dynamics. . . . .	6
Figure 2. $\text{NO}(v=1, J \approx 12\frac{1}{2})$ image obtained following photodissociation of $\text{NO}_2$ . . . . .	8
Figure 3. Image of Figure 2, rotated $5^\circ$ cw and symmetrized . . . . .	8
Figure 4. Image transformed to provide the three-dimensional velocity distribution. . . . .	9
Figure 5. Angular distribution of $\text{NO}(v=1, J \approx 12\frac{1}{2})$ . . . . .	9
Figure 6. Image obtained monitoring $\text{NO}(v=1, J=20\frac{1}{2})$ . . . . .	10
Figure 7: Methyl velocity distribution from dissociation of nitromethane at 193 nm. . . . .	11
Figure 8. Rotational Distribution of $\text{NO}(X)$ product of $\text{CH}_3\text{NO}_2$ Photodissociation . . . . .	11
Figure 9. Rydberg series ionization spectrum of $\text{NO}(A)$ produced by secondary photolysis of $\text{CH}_3\text{NO}_2$ . . . . .	12

**A. Statement of the Problem Studied**

A new technique for characterizing the velocity distributions of state-selected reaction products was developed for analyzing the reactions of hydrogen atoms: the three dimensional velocity distribution of product fragments is determined by ionizing the appropriate species, waiting for a delay while the species separate along their trajectories, and then projecting the spatial distribution of ions onto a two-dimensional screen. The objectives of this work were to develop the new technique and, eventually, to apply it to use it in order to characterize the reactions of hydrogen atoms with  $\text{NO}_2$ ,  $\text{CH}_3\text{HNO}_2$ , and  $\text{H}_2\text{NNO}_2$ .

**B. Summary of the Most Important Results**

An important goal of this work has been to develop further the experimental imaging technique for measuring three-dimensional velocity distributions of reaction or photodissociation products. In this technique, invented in collaboration with David Chandler,<sup>1</sup> products are first state-selected by resonance-enhanced multiphoton ionization and are then allowed to recoil in a field-free region according to their original velocities. After a suitable time delay, the three dimensional spatial distribution corresponding to the velocity distribution is projected onto a two-dimensional surface by applying an electrical acceleration to the ions. If the projection is made in a direction perpendicular to a dynamical axis of cylindrical symmetry, such as the polarization vector of the dissociating light for a photodissociation or the relative velocity vector for a reaction, then a straightforward transform can recover the three-dimensional velocity distribution from the two-dimensional image.<sup>2,3</sup>

Development of the imaging technique has proceeded simultaneously at Sandia and at Cornell. The Chandler group has been extremely successful in using the method to investigate the photodissociations of  $\text{CH}_3\text{I}$ ,  $\text{CH}_3\text{Br}$ , and  $\text{H}_2\text{S}$ .<sup>4-7</sup> Our own efforts have been aimed at constructing a somewhat different version of the apparatus, one that is specifically suited to studying the above-mentioned reactions.

### 1. Apparatus Construction

We describe here the molecular beam/ion imaging apparatus which has been constructed in our laboratory. Figure 1 displays a schematic diagram of the instrument, which is based on a modified Wiley-McLaren time-of-flight mass spectrometer.<sup>8</sup> The molecular beam source and differential pumping stage, neither of which is shown in the schematic, are used to produce and collimate a pulsed molecular beam

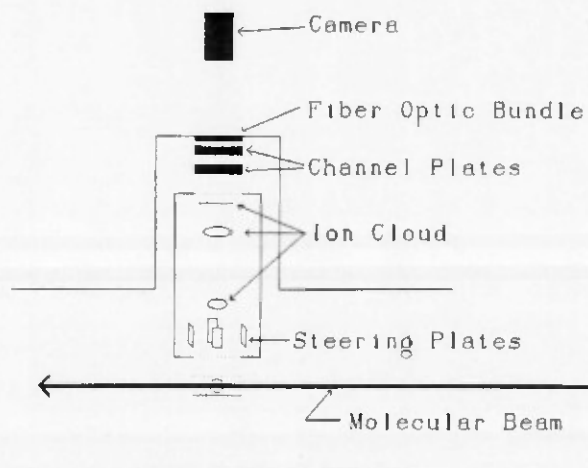


Figure 1. Single molecular beam apparatus used for studies of photodissociation dynamics.

whose diameter at the interaction region is about 1.5 mm. For photolysis studies, the beam is crossed in the interaction region by pulsed radiation from two laser systems. The first pulse is used to dissociate the parent molecule, for example  $\text{NO}_2$  (see below), while the second pulse is used to ionize a selected state of the fragment, for example NO. At this point, there is zero field on the repeller plates and grids of the spectrometer, so the fragments, now ions, move forward with the molecular beam velocity and recoil outward from their center of mass with the velocity imparted by the dissociation; the ejected electron is too light to have an appreciable influence on the recoil velocities. After a suitable time delay, a field of 100-500 volts/cm is applied to accelerate the ion "cloud" upward. The forward velocity is counteracted, if needed, by applying small voltages to the steering plates. Note that because of the design of the Wiley-McLaren instrument, ions originally flying downward are accelerated for a longer time than those flying upward. If the voltages on the grids and plates are properly adjusted, the ion cloud will be focused as suggested in Figure 1, which shows the shape of the cloud at different times during its flight. For optimal conditions, the cloud becomes a "pancake" just as it hits the channeltron detector, which is located 52 cm from the interaction zone.

It should be noted that the design described above differs from that of the original apparatus<sup>1</sup> and from that currently used at Sandia.<sup>4-7</sup> Our apparatus accelerates the ions in a direction



perpendicular to the molecular beam rather than down the axis of the beam. There are two reasons for choosing this geometry. The first is that it allows us to ensure that nearly all of the ions hit the channel plate at the same time, so that possible blurring of the image due to different ion arrival times can be minimized. The second reason is that this geometry allows us to add a second molecular beam source and to still have the projection direction perpendicular to the relative velocity vector for the reactants. This arrangement is important, because one projection is sufficient for calculation of the full three-dimensional velocity distribution only when the projection is made in a direction perpendicular to an axis of cylindrical symmetry, such as the relative velocity vector or the polarization vector of a photodissociation laser.

The channeltron pair of Figure 1 with its integral fiber optic bundle was built to our specifications by Galileo Electro-Optics Corporation. The channels are 12  $\mu\text{m}$  in diameter separated by 15  $\mu\text{m}$  (center-to-center), and the pair of plates produces a gain of up to  $7 \times 10^6$ . Behind each point where an ion strikes the detector, the amplified electrons are accelerated into the fiberoptic bundle, whose end is coated with a fast phosphor (P47, 80 ns response). The bundle is fed through a flange in the vacuum chamber, and the image, now a two-dimensional projection of the three-dimensional spatial distribution, is photographed with a charge-injection device (CID) camera (Xybion Electronic Systems) equipped with a 512x512 pixel array and a gated intensifier. The intensifier is gated to capture only the mass of interest. Finally, the image is sent to a computer/averager system formed from hardware purchased from Poynting Products, Inc. and IBM. We can average 128 shots into each of 17 stored images at 10 Hz in real time using a hard-wired, 16 bit averager. Following every  $128 \times 17 = 2176$  shots, the averaged data is added into computer memory, where additional software averaging can be performed if required. Images are manipulated on the laboratory computer system and then sent to an IBM PS/2 or a mainframe computer for further analysis.

Because we know both the position of each ion on the screen and the arrival time of the pancake, the two-dimensional spatial projection is easily converted to a two-dimensional velocity

projection. When the projection has been made in a direction perpendicular to an axis of cylindrical symmetry, it is possible to calculate the full three-dimensional velocity distribution from one two-dimensional projection using, for example, a Hankel transform.<sup>2,3,9</sup> The procedure is illustrated in the next section where we present data obtained on our instrument for the photodissociation of  $\text{NO}_2$ .

## 2. $\text{NO}_2$ Photodissociation

Although the photodissociation of  $\text{NO}_2$  at wavelengths from 200–400 nm has been studied by several previous groups,<sup>10–14</sup> the angular distribution of state-resolved NO photofragments has been performed in only limited spectral regions. In order both to test our apparatus and to learn some new information about this interesting dissociation, we have performed measurements of the  $\text{NO}(v, J)$  product angular distributions following dissociation of  $\text{NO}_2$  at 355 nm using a tripled YAG laser. Figure 2 shows the image obtained probing  $\text{NO}(v=1, J \approx 12\frac{1}{2})$  by 1+1 multiphoton ionization, where the polarization vector of the dissociating light is parallel to the vertical direction in the diagram. In agreement with the findings of Busch and Wilson for non-state-resolved products at 347.1 nm,<sup>11</sup> the raw data demonstrates that the angular distribution is produced from a predominantly parallel transition. A more quantitative measure can be obtained by the following procedure. Since the photodissociation produces a symmetric distribution with respect to both

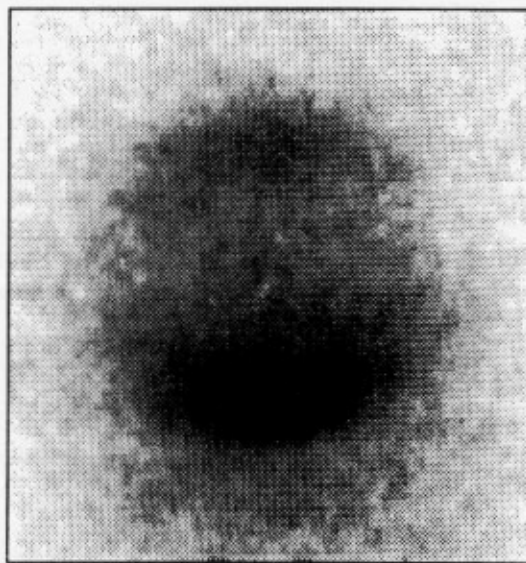


Figure 2.  $\text{NO}(v=1, J \approx 12\frac{1}{2})$  image obtained following photodissociation of  $\text{NO}_2$

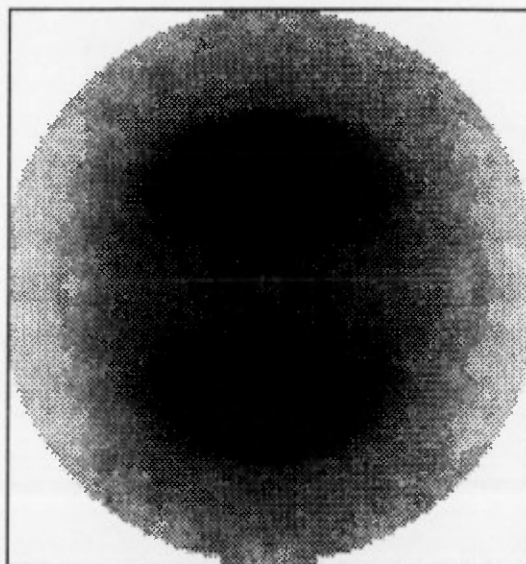


Figure 3. Image of Figure 2, rotated  $5^\circ$  cw and symmetrized

vertical and horizontal planes, the data can be averaged and symmetrized to produce the image shown in Figure 3, which compensates for the laser and detector inhomogeneities which cause the asymmetry in Figure 2. Inversion<sup>2,3</sup> of this two-dimensional projection can be performed in order to obtain the three-dimensional velocity distribution shown in Figure 4, which provides the density of photo-fragments at a particular speed (given by the position of the density with respect to the center) and at a given angle. The three-dimensional distribution is cylindrically symmetric about the vertical axis. By integrating over speed at fixed angles, we can obtain the angular distribution, or by integrating over angles at fixed speed, we can obtain the speed distribution. The former is characterized by an anisotropy parameter  $\beta=0.71$  (in  $I(\theta) \propto [1 + \beta P_2(\cos\theta)]$ ), as shown in Figure 5. This value is in reasonable agreement with the value of  $\beta=0.74$  obtained by Busch and Wilson at 347.1 nm averaging over the entire NO vibrational-rotational distribution. The speed distribution is characterized by a gaussian centered at a speed of 425 m/s, consistent with conservation of energy constraints for  $\text{NO}(v=1, J \approx 12\frac{1}{2}) + \text{O}(^3\text{P}_2)$  to within our resolution.

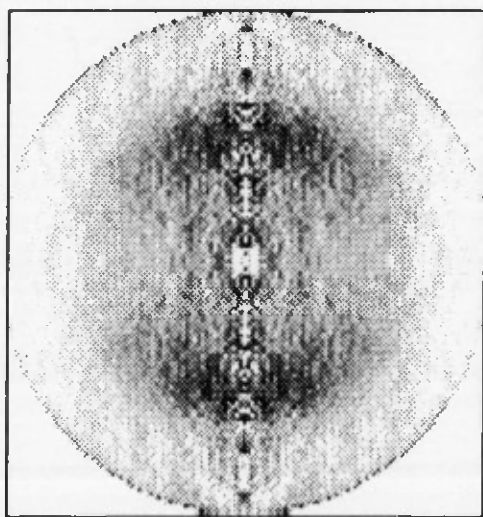


Figure 4. Image transformed to provide the three-dimensional velocity distribution.

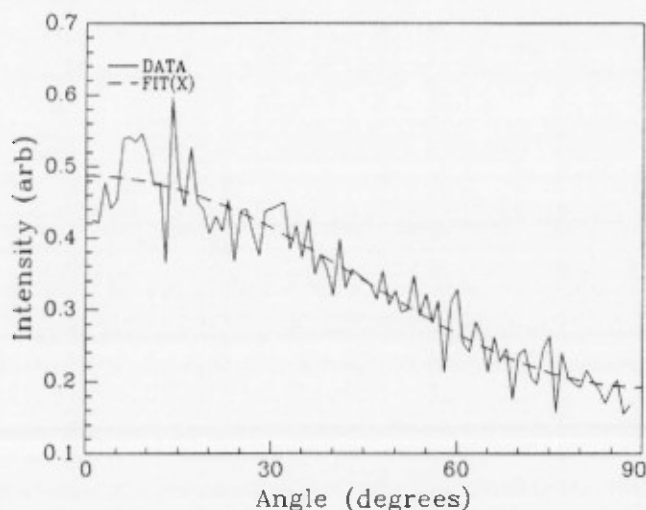


Figure 5. Angular distribution of  $\text{NO}(v=1, J \approx 12\frac{1}{2})$ .

An interesting phenomenon occurs if we tune our probe laser to monitor  $\text{NO}(\nu=1, J \approx 20\frac{1}{2})$ . The image, shown in Figure 6, appears to correspond to a perpendicular transition. The data no longer shows the double lobe structure of Figure 2 and Figure 3 but rather shows a single, central spot as if the products recoiled perpendicular to the polarization vector of the dissociating light. Although this result is preliminary, it may indicate that the dissociation is more complex than previously assumed. In particular, one can reasonably question why the apparent anisotropy should

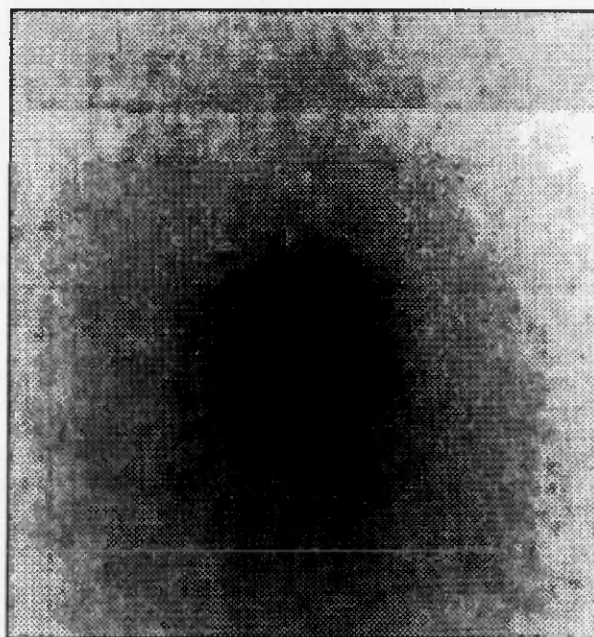
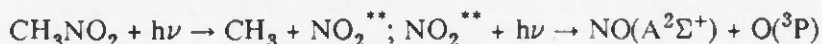
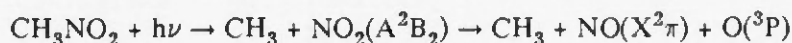


Figure 6. Image obtained monitoring  $\text{NO}(\nu=1, J=20\frac{1}{2})$ .

change so dramatically with product internal energy. The ability of this technique to measure velocity distributions for state-selected products will be an important advantage in this and other studies.

### 3. $\text{CH}_3\text{NO}_2$ Photodissociation

We have also performed an investigation of the photodissociation of  $\text{CH}_3\text{NO}_2$  by measuring the internal and translational energy distributions of all products. This molecule is of some interest to the Army mission because of its structural similarity to other nitro-containing compounds. Our results are consistent with and complementary to those presented by Butler *et al.*,<sup>15</sup> who measured the translational energy distributions and the fluorescence emission spectrum of the  $\text{NO}_2^{**}$  product, where the double star notation indicates an excited electronic state. We have determined the internal and translational energy distributions for the  $\text{CH}_3$ ,  $\text{NO}(\text{X})$ ,  $\text{NO}(\text{A})$ , and  $\text{O}(^3\text{P})$  products. Our results support the following two pathways for the 193-nm photolysis of nitromethane:



The significant results and conclusions which support this mechanism are as follows: 1) We observe a methyl product with relatively little internal excitation and with a translational energy distribution indicative of two dissociation pathways, as shown in Figure 7. 2) We observe secondary dissociation products  $\text{NO}(\text{X}$  and  $\text{A})$  and  $\text{O}(^3\text{P})$ , with relatively little translational energy. The  $\text{NO}(\text{X})$  product has a rotational temperature

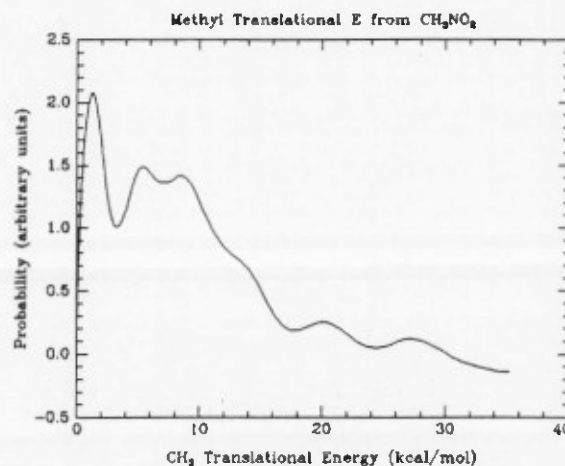


Figure 7: Methyl velocity distribution from dissociation of nitromethane at 193 nm.

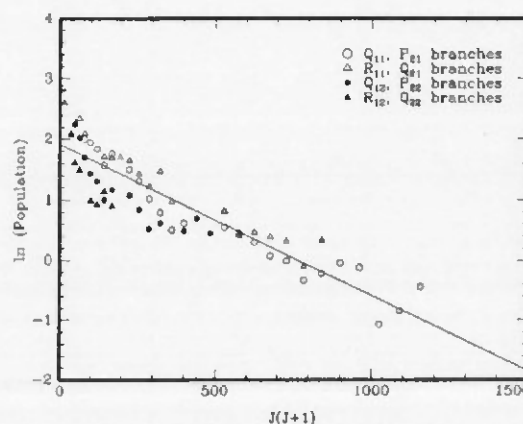


Figure 8. Rotational Distribution of  $\text{NO}(\text{X})$  product of  $\text{CH}_3\text{NO}_2$  Photodissociation

of  $1000 \pm 100$  K, as shown in Figure 8, and is primarily formed in  $v=0$ . The NO(A) product is formed as a result of secondary photodissociation of NO<sub>2</sub>. We observe it by 1+1 ionization of NO(A) through a Rydberg series of transitions, as shown in Figure 9. 3) An impulsive model of the CH<sub>3</sub>NO<sub>2</sub> dissociation fits the observed partitioning of energy among the fragments from the major channel, while the minor NO<sub>2</sub> dissociation channel, involving the absorption of a second 193-nm photon, is not well described by such a model.

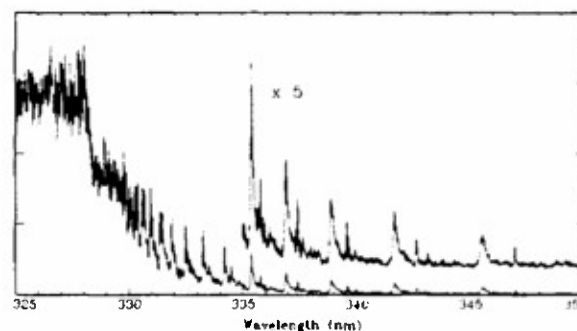


Figure 9. Rydberg series ionization spectrum of NO(A) produced by secondary photolysis of CH<sub>3</sub>NO<sub>2</sub>.

#### 4. Crossed Molecular Beam Apparatus

While testing the single beam imaging apparatus by investigating the photodissociations of NO<sub>2</sub> and CH<sub>3</sub>NO<sub>2</sub>, we have begun construction of another beam source so that we can explore inelastic and reactive collisions by imaging the differential cross sections for state-selected products. The source has two configurations, one for forming a beam of stable atoms or molecules and a second for producing a beam of unstable species, hydrogen atoms for example. The first configuration is very similar to the source chamber for the primary beam and is pumped by a 6 inch diffusion pump (Varian VHS-6) backed by a 765 l/min rotary pump. The beam source consists of a pulsed nozzle (Precision Instrument Services), a skimmer of 1.0 mm diameter, and a short connector so that the beam can be aligned to intersect the primary source in the interaction region shown in Figure 1. The flange separating the secondary source from the interaction zone is equipped with optical windows for entering and exiting laser beams.

**C. List of All Publications and Technical Reports**

1. V. Hradil, C. E. M. Strauss, and P. L. Houston, "Direct imaging of the CO product of 230-nm OCS Photodissociation," in preparation
2. V. Hradil, T. Suzuki, S. Hewitt, L. Bontuyan, and P. L. Houston, "Investigation of the Photodissociation dynamics of NO<sub>2</sub> at 355 nm using Imaging of the Velocity Distributions for State-Selected NO Products," in preparation.

**D. List of All Participating Scientific Personnel**

Paul L. Houston (principal investigator)  
Vincent Hradil (graduate student)  
Scott Hewitt (postdoctoral associate)  
Toshinori Suzuki (visiting scientist from Japan)  
Lizla Bontuyan (graduate student)  
Benjamin Whitaker (visiting scientist from Leeds University, UK)

**E. Report of Inventions**

There were no inventions for this project during the grant period.

**F. Bibliography**

1. D. W. Chandler and P. L. Houston, "Velocity and Internal State Distributions by Two-Dimensional Imaging of Products Detected by Multiphoton Ionization," *J. Chem. Phys.* **87**, 1445 (1987).
2. L. A. Shepp and B. F. Logan, *IEEE Trans. Nuc. Sci.* **NS-21**, 21 (1974).
3. K. R. Castleman, *Digital Image Processing*, (Prentice-Hall, 1979), pp. 184-185.
4. J. W. Thoman, D. W. Chandler, D. H. Parker, and M. H. M. Janssen, *Laser Chem.* **9**, 27 (1988).
5. D. W. Chandler, J. W. Thoman, G. O. Sitz, M. H. M. Janssen, S. Stolte, and D. H. Parker, *J. Chem. Soc., Faraday Trans 2* **85**, 1305 (1989).
6. D. W. Chandler, J. W. Thoman, M. H. M. Janssen, and D. H. Parker, *Chem. Phys. Lett.* **156**, 151 (1989).
7. D. H. Parker, Z. W. Wang, M. H. M. Janssen, and D. W. Chandler, *J. Chem. Phys.* **90**, 60 (1989).
8. W. C. Wiley and I. H. McLaren, *Rev. Sci. Instrum.* **26**, 1150 (1955).

9. We assume for the purposes of discussion here that the ionizing step does not depend on the alignment of the fragments. Interesting information about the correlation of the velocity  $v$  and the rotation vector  $J$  of the fragments can be obtained by observing how the image changes with the relative polarization of the laser used for multiphoton ionization.
10. G. E. Busch and K. R. Wilson, *J. Chem. Phys.* **56**, 3626 (1972).
11. G. E. Busch and K. R. Wilson, *J. Chem. Phys.* **56**, 3638 (1972).
12. H. Zacharias, M. Geilaupt, K. Meier, and K. H. Welge, *J. Chem. Phys.* **74**, 218 (1981).
13. M. Kawasaki, H. Sato, A. Fukuroda, T. Kikuchi, S. Kobayashi, and T. Arikawa, *J. Chem. Phys.* **86**, 4431 (1987).
14. M. Mons and I. Dimicoli, *Chem. Phys.* **130**, 307 (1989).
15. L. J. Butler, D. Krajnovich, Y. T. Lee, G. Ondrey, and R. Bersohn, *J. Chem. Phys.* **79**, 1708 (1983).